ON THE EXPERIMENTAL REALISATION OF MULTI-AXIAL STRESS STATES FOR CELLULAR AND POROUS MATERIALS: DETERMINATION OF ELASTO-PLASTIC PROPERTIES

Andreas Öchsner
Department of Mechanical Engineering, Centre for Mechanical Technology and Automation, University of Aveiro, Portugal
aoechsner@mec.ua.pt

Thomas Fiedler
Centre for Mechanical Technology and Automation, University of Aveiro, Portugal
tfiedler@mec.ua.pt

José Grácio
Department of Mechanical Engineering, Centre for Mechanical Technology and Automation, University of Aveiro, Portugal
jgracio@mec.ua.pt

Abstract. *The determination of the yield surface of cellular and porous materials requires experimental procedures under multi-axial stress states as the yield behaviour is sensitive to the hydrostatic stress and as simple uniaxial tests aim only to determine one single point of the yield surface. Therefore, an experimental technique based on a plane strain test and a technique based on a uniaxial strain test for the description of the elastic-plastic transition zone at small strains are proposed. These experiments can be achieved in a biaxial testing machine or in a tube. Simple cubic models of periodic cellular metals are used to demonstrate the method for materials of different relative densities. In contrast to common analytical and numerical models, experimental samples of the same geometry are easy to manufacture and to simulate. Furthermore, these experimental techniques enable the determination of Poisson's ratio in the elastic range. The experimental procedure is verified by the finite element method.*

Keywords: *multi-axial testing, cellular solids, plasticity, yield surface, nonlinear behaviour*

1. Introduction

Cellular metals and porous materials, e.g. metal foams (cf. Fig. 1), exhibit unique mechanical and physical properties that differ strongly from classical solid materials and are currently being considered for use in lightweight structures such as cores of sandwich panels or as passive safety components of automobiles, (Gibson and Ashby, 1997). Interesting combinations of their mechanical and physical properties, such as relatively high stiffness in conjunction with very low weight or high gas permeability combined with high thermal conductivity, offer the possibility for new future-oriented multifunctional applications, e.g. in aviation and space technology.

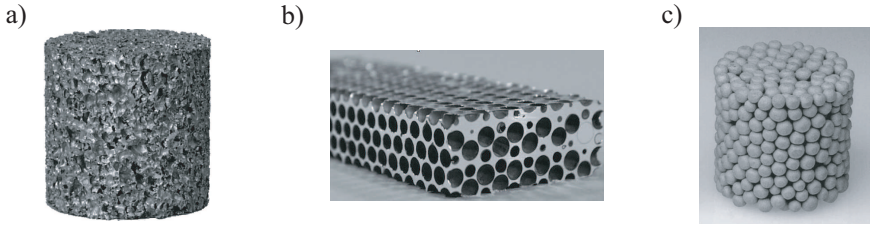

Figure 1. Different types of cellular materials: a) closed-cell metal foam (ALPORAS®); b) hollow alumina spheres embedded in a magnesium matrix; c) hollow sphere foam $Fe_{0.88}Cr_{0.12}$; (Körner and Singer, 2000)

The mechanical properties of cellular metals, in particular their resistance to plastic deformation, the evolution and progress of damage and fracture within the material, are determined by the microstructure and the cell wall material, respectively. The most important structural parameters which characterise a cellular metal are the morphology of the cell (geometry, open- or closed-cell), the topology, the mean cell size and the relative density ϱ/ρ_S (the macroscopic density ϱ divided by that of the solid material of the cell wall ϱ_S, (Ashby et al. (2000)). However, there are still technological problems related to the control of the structure and properties of the cellular material, which remain to be solved. The vast majority of existing techniques do not allow for precise control of shape, size and distribution of the pores. That brings about a wide scatter in mechanical and other characteristics of the materials and components. The experimental determination of material properties of cellular materials is quite complicated since classical extensometers or strain gauges are

difficult to attach on the cellular surface which is extremely rough and structured. Young's modulus and the (uniaxial) flow curve can be determined based on classical uniaxial tensile or compression tests. However, the determination of a second elastic constant, e.g. Poisson's ratio, is extremely diffcult to realise because the measurement of the transversal strains with classical methods is not possible. A plane strain state realised due to a biaxial testing machine is proposed in the following. However, the realisation is connected with complex and expensive experimental equipment and might be not available in standard test laboratories. Therefore, a method based on an axial compaction test which is easy to realise in a universal testing machine is proposed as a second method and alternative. These tests aims not only to determine a second elastic constant but also the parameters of the yield criterium. The methods are verified based on regular model structures by numerical simulation.

2. General description of yield criteria for cellular and porous materials

A commonly used constitutive equation for foamed materials was developed based on experimental investigations of metallic (Deshpande and Fleck, 2000) and polymer foams (Deshpande and Fleck, 2001). A mathematical formulation of the form

$$F = \frac{1}{\left[1 + \left(\frac{\alpha}{3}\right)^2\right]} \cdot \left[\sigma_{\mathrm{e}}^2 + \alpha^2 \sigma_{\mathrm{m}}^2\right] - k_{\mathrm{t}}^2 = 0 \tag{1}$$

has been proposed where $\sigma_{\mathrm{m}} = \frac{1}{3}\left(\sigma_x + \sigma_y + \sigma_z\right) = \frac{1}{3} \cdot J_1^{\mathrm{o}}$ is the mean stress and $\sigma_{\mathrm{e}} = \sqrt{\frac{3}{2} s_{ij} s_{ij}} = \sqrt{3 J_2'}$ is the von Mises effective stress. Parameter α and the uniaxial tensile yield stress k_{t} are functions of some internal variable. The effective plastic strain $\varepsilon_{\mathrm{eff}}^{\mathrm{p}}$ may serve as this internal variable. Thus, dependencies of the form $\alpha = \alpha(\varepsilon_{\mathrm{eff}}^{\mathrm{p}})$ and $k_{\mathrm{t}} = k_{\mathrm{t}}(\varepsilon_{\mathrm{eff}}^{\mathrm{p}})$ are obtained. In the definition of the mean and effective stress, the first invariant $J_1^{\mathrm{o}} = \sigma_{ii}$ of the spherical stress tensor σ_{ij}^{o} and the second invariant $J_2' = \frac{1}{2}\, s_{ij} s_{ij}$ of the deviator stress tensor s_{ij} have been introduced. Thus, the yield criterion (1) can be rearranged to obtain:

$$F = \frac{3}{1 + \frac{\alpha^2}{9}} \cdot J_2' + \frac{\frac{1}{9}\alpha^2}{1 + \frac{\alpha^2}{9}} \cdot \left(J_1^{\mathrm{o}}\right)^2 - k_{\mathrm{t}}^2 = 0\,. \tag{2}$$

The graphical representation of this yield criterion is shown in Fig. 2 in different spaces.

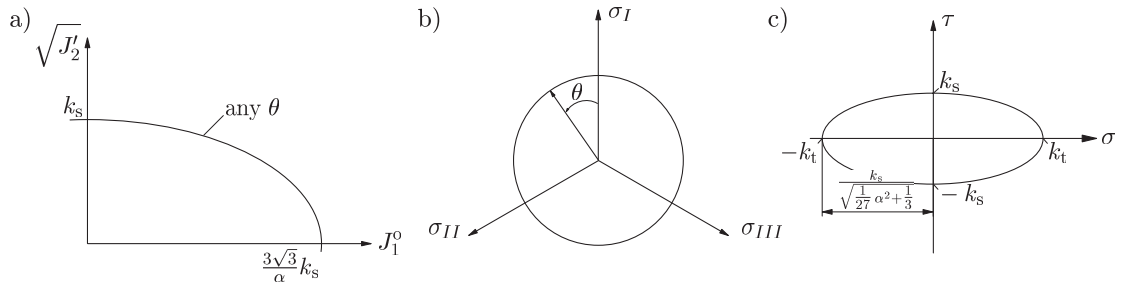

Figure 2. Graphical representation of the yield condition according to Deshpande-Fleck: a) $\sqrt{J_2'} - J_1^{\mathrm{o}}-$ coordinate system; b) octahedral plane; c) $\sigma - \tau-$ space

It might be more appropriate for the mathematical treatment to replace the tensile yield stress k_{t} by the shear stress k_s. To this end, a $\sigma - \tau$ stress space is considered. This stress space is defined by a single normal stress σ and a single shear stress τ (cf. Fig. 2 c)). The invariants reduces in such a stress space to $J_1^{\mathrm{o}} \rightarrow \sigma$ and $J_2' \rightarrow \frac{1}{3}\sigma^2 + \tau^2$. Introducing these definitions into Eq. (2) results in the yield criterion in the $\sigma - \tau$ stress space as:

$$F_{\sigma-\tau} = \frac{3}{1 + \frac{\alpha^2}{9}} \cdot \left(\frac{1}{3}\sigma^2 + \tau^2\right) + \frac{\frac{1}{9}\alpha^2}{1 + \frac{\alpha^2}{9}} \cdot \sigma^2 - k_{\mathrm{t}}^2 = 0\,. \tag{3}$$

The relationship between the tensile and shear yield stress follows then from the conditions $\sigma \rightarrow 0 \;\; \Rightarrow \;\; \tau \rightarrow k_{\mathrm{s}}$ as

$$\frac{3}{1 + \frac{\alpha^2}{9}} k_{\mathrm{s}}^2 = k_{\mathrm{t}}^2\,. \tag{4}$$

Introducing this relationship between the tensile and shear yield stress into Eq. (2) gives finally:

$$F = \frac{1}{27} \cdot \alpha^2 \left(J_1^{\mathrm{o}}\right)^2 + J_2' - k_{\mathrm{s}}^2 = 0\,, \tag{5}$$

which is much more appropriate for mathematical transformations.
Equation (5) can generally be expressed in the form

$$F = g_1(\alpha) \cdot f_1(J_1^{\mathrm{o}}) + f_2(J_2') + f_3(k_{\mathrm{s}}) = 0, \tag{6}$$

where $f_i (i = 1, 2, 3)$ and g_1 are arbitrary scalar functions. The general form (6) includes many different yield criterions. Some examples are given in Tab. 1.

Table 1. Yield criteria of the form (6).

g_1	f_1	f_2	f_3
Deshpande and Fleck, 2000, 2001			
$\frac{1}{27}\alpha^2$	$\left(J_1^{\mathrm{o}}\right)^2$	J_2'	k_{s}^2
Mahrenholtz and Ismar, 1979, 1981			
α	$\left(J_1^{\mathrm{o}}\right)^2$	J_2'	k_{s}^2
Drucker and Prager			
α	J_1^{o}	$\sqrt{J_2'}$	k_{s}
von Mises			
0	0	$\sqrt{J_2'}$	k_{s}

It should be noted here that the same dependency of the yield criterion on the stress invariants J_1^{o} and $J_2^{'}$ as in Eq. (5) has been obtained by accurate finite element simulations on periodic polyhedron cells in (Ströhla, Winter and Kuhn, 2003) for open-cell and in (Ströhla, Winter and Kuhn, 2003) for closed-cell metal foams.

The experimental task is now the determination of the parameter α and the yield stress k_{s} (or k_{t}). While the uniaxial yield stress k_{t} can be determined for example based on uniaxial tensile or compression tests, the measurement of α is much more complicated. In the following, a plane strain and a uniaxial strain (axial compaction) state is considered to determine both parameters.

3. States of uniaxial strain and plane stress

Under the classical assumption of small strains, the total strain increment $\mathrm{d}\varepsilon_{ij}$ is assumed to be the sum of the elastic strain increment $\mathrm{d}\varepsilon_{ij}^{\mathrm{e}}$ and the plastic strain increment $\mathrm{d}\varepsilon_{ij}^{\mathrm{p}}$

$$\mathrm{d}\varepsilon_{ij} = \mathrm{d}\varepsilon_{ij}^{\mathrm{e}} + \mathrm{d}\varepsilon_{ij}^{\mathrm{p}}\,, \tag{7}$$

where the elastic strain increment can be obtained from Hooke's law

$$\varepsilon_{ij} = \frac{1+\nu}{E}\left(\sigma_{ij} - \frac{\nu}{1+\nu}\delta_{ij}\sigma_{kk}\right) = C_{ijkl}^{-1}\sigma_{kl}\,, \tag{8}$$

and the plastic strain increment from the associated flow rule

$$\mathrm{d}\varepsilon_{ij}^{\mathrm{p}} = \mathrm{d}\lambda\frac{\partial F}{\partial \sigma_{ij}}. \tag{9}$$

Application of the chain rule with respect to the stress tensor σ_{ij} gives the derivative of the general scalar yield criterion (6) as:

$$\frac{\partial F}{\partial \sigma_{ij}} = \frac{\partial F}{\partial J_1^{\mathrm{o}}}\frac{\partial J_1^{\mathrm{o}}}{\partial \sigma_{ij}} + \frac{\partial F}{\partial J_2'}\frac{\partial J_2'}{\partial \sigma_{ij}} = g_1(\alpha)\frac{\partial f_1}{\partial J_1^{\mathrm{o}}}\cdot\delta_{ij} + \frac{\partial f_2}{\partial J_2'}\cdot s_{ij}\,. \tag{10}$$

The terms $\partial F/\partial J_1^{\mathrm{o}}$ and $\partial F/\partial J_2'$ are normally simple derivatives of polynomial expressions.

In the following, only the yield criterion according to Eq. (5) is considered. The derivative of F with respect to the stress tensor σ_{ij} is obtained in this case as:

$$\frac{\partial F}{\partial \sigma_{ij}} = \frac{2}{27}\alpha^2\cdot J_1^{\mathrm{o}}\cdot\delta_{ij} + 1\cdot s_{ij}\,. \tag{11}$$

If Hooke's law (8) is applied for the elastic component and the associated flow rule (9) for the plastic component, the complete stress-strain relationship for a material obeying a yield criterium of form (5) is expressed as

$$\mathrm{d}\varepsilon_{ij} = \frac{1+\nu}{E}\left(\mathrm{d}\sigma_{ij} - \frac{\nu}{1+\nu}\delta_{ij}\mathrm{d}\sigma_{kk}\right) + \mathrm{d}\lambda\left(\frac{2}{27}\alpha^2\cdot J_1^{\mathrm{o}}\cdot\delta_{ij} + 1\cdot s_{ij}\right)\,. \tag{12}$$

For a state of plane strain (no wall friction, principal directions are I, II, III), we have (cf. Fig. 3 a))

$$\sigma_I < 0 \quad\wedge\quad \varepsilon_I \neq 0\,, \tag{13}$$
$$\sigma_{II} \neq 0 \quad\wedge\quad \varepsilon_{II} = 0\,, \tag{14}$$
$$\sigma_{III} = 0 \quad\wedge\quad \varepsilon_{III} \neq 0\,, \tag{15}$$

while a state of uniaxial strain (cf. Fig. 3 b)) is characterised by (13), (14) and $\sigma_{III} \neq 0 \quad\wedge\quad \varepsilon_{III} = 0$.

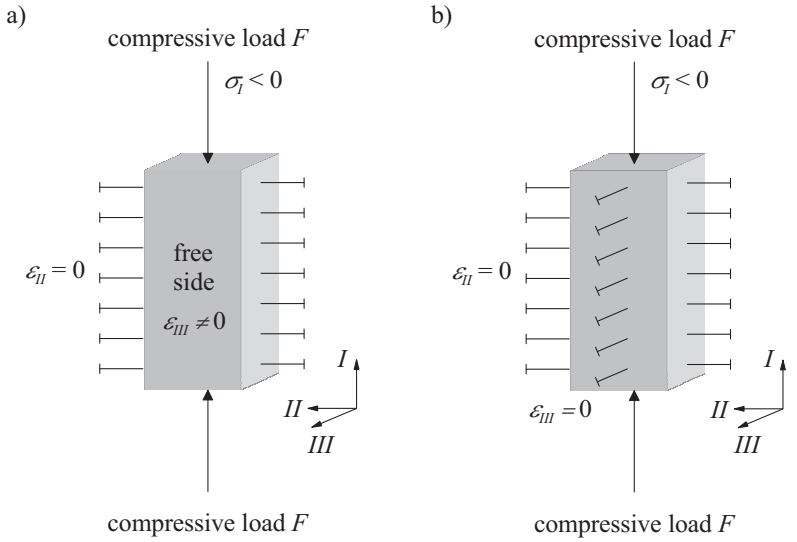

Figure 3. Schematic representation of a state of plane strain a) and a state of uniaxial strain b)

Using Eqs. (13)-(15) with the associated flow rule (9) and (12), the increments of the plastic strain are given for principal stresses by:

$$\mathrm{d}\varepsilon_I^{\mathrm{p}} = \mathrm{d}\lambda\left[\frac{2}{27}\alpha^2(\sigma_I + \sigma_{II} + \kappa\sigma_{III}) + \frac{1}{3}(2\sigma_I - \sigma_{II} - \kappa\sigma_{III})\right]\,, \tag{16}$$

$$\mathrm{d}\varepsilon_{II}^{\mathrm{p}} = \mathrm{d}\lambda\left[\frac{2}{27}\alpha^2(\sigma_I + \sigma_{II} + \kappa\sigma_{III}) + \frac{1}{3}(-\sigma_I + 2\sigma_{II} - \kappa\sigma_{III})\right]\,. \tag{17}$$

where the parameter κ distinguishes between the plane strain ($\kappa = 0$) and uniaxial strain ($\kappa = 1$) case:
Dividing Eq. (17) by (16) and rearranging for α yields to an equation of the form

$$\alpha^2 = \frac{9}{2} \cdot \frac{\sigma_I \left(1 + 2\frac{\mathrm{d}\varepsilon^{\mathrm{p}}_{II}}{\mathrm{d}\varepsilon^{\mathrm{p}}_{I}}\right) - \sigma_{II}\left(2 + \frac{\mathrm{d}\varepsilon^{\mathrm{p}}_{II}}{\mathrm{d}\varepsilon^{\mathrm{p}}_{I}}\right) + \kappa\sigma_{III}\left(1 - \frac{\mathrm{d}\varepsilon^{\mathrm{p}}_{II}}{\mathrm{d}\varepsilon^{\mathrm{p}}_{I}}\right)}{(\sigma_I + \sigma_{II} + \kappa\sigma_{III})\left(1 - \frac{\mathrm{d}\varepsilon^{\mathrm{p}}_{II}}{\mathrm{d}\varepsilon^{\mathrm{p}}_{I}}\right)}. \tag{18}$$

For small plastic strains (respectively at the beginning of the yielding), the quotient is $\mathrm{d}\varepsilon^{\mathrm{p}}_{II}/\mathrm{d}\varepsilon^{\mathrm{p}}_{I} \ll 1$ (respectively = 0) and the quantity α can be approximated by

$$\alpha^2 \approx \frac{9}{2} \cdot \frac{\sigma_I - 2\sigma_{II} + \kappa\sigma_{III}}{\sigma_I + \sigma_{II} + \kappa\sigma_{III}}. \tag{19}$$

Evaluation of Eq. (18) requires the determination of the plastic strain increments $\mathrm{d}\varepsilon^{\mathrm{p}}_{I}$ and $\mathrm{d}\varepsilon^{\mathrm{p}}_{II}$. These increments can be determined from Eq. (7) as

$$\mathrm{d}\varepsilon^{\mathrm{p}}_{I} = \mathrm{d}\varepsilon_I - \mathrm{d}\varepsilon^{\mathrm{e}}_{I}\,, \tag{20}$$

$$\mathrm{d}\varepsilon^{\mathrm{p}}_{II} = \underbrace{\mathrm{d}\varepsilon_{II}}_{=0} - \mathrm{d}\varepsilon^{\mathrm{e}}_{II} = -\mathrm{d}\varepsilon^{\mathrm{e}}_{II}\,, \tag{21}$$

$$\mathrm{d}\varepsilon^{\mathrm{p}}_{III} \begin{cases} \kappa = 1: & \underbrace{\mathrm{d}\varepsilon_{III}}_{=0} - \mathrm{d}\varepsilon^{\mathrm{e}}_{III} = -\mathrm{d}\varepsilon^{\mathrm{e}}_{III}\,, \\ \kappa = 0: & \mathrm{d}\varepsilon_{III} - \mathrm{d}\varepsilon^{\mathrm{e}}_{III}\,, \end{cases} \tag{22}$$

while the elastic strain increments can be obtained from Hooke's law (8).

It should be noted here that in the case of a uniaxial stress state ($\sigma_{II} = \sigma_{III} = 0$), Eqs. (16) and (17) can be reduced to [3]

$$-\frac{\mathrm{d}\varepsilon^{\mathrm{p}}_{II}}{\mathrm{d}\varepsilon^{\mathrm{p}}_{I}} = \frac{(1/2) - (\alpha/3)^2}{1 + (\alpha/3)^2}. \tag{23}$$

However, Eq. (23) is difficult to apply in experimental practice for the determination of α since the lateral strains are extremely hard to measure.

In the hardening theory of plasticity, the hardening parameter in the yield criterion must be related to the experimental uniaxial stress-strain curve. To this end, one needs to define a stress variable, called effective stress, which is a function of the stresses and some strain variables, called effective strain, which is a function of the plastic strains, so that they can be plotted and used to correlate the test results obtained by different loading conditions, (Chen and Hahn, 1988). Since the effective stress should reduce to the stress σ_I in a uniaxial test, it follows that the function $f = g_1(\alpha) \cdot f_1(J^{\mathrm{o}}_1) + f_2(J'_2)$ must be some constant c multiplied by the effective stress σ_{eff} to some power n, i.e. $f(\sigma_{ij}, \varepsilon^{\mathrm{p}}_{\mathrm{eff}}) = c \cdot \sigma^{\mathrm{n}}_{\mathrm{eff}}$. For the uniaxial test with $\sigma_{\mathrm{eff}} = \sigma_I$, $\sigma_{II} = \sigma_{III} = 0$ and $J^{\mathrm{o}}_1 = \sigma_I$; $J'_2 = \frac{1}{3}\sigma^2_I$, coefficient comparison, i.e. $g_1(\alpha) f_1(\sigma_I) + f_2(\sigma_I) = c \cdot \sigma^n_I$, gives the parameters c and n. The effective plastic strain increment $\mathrm{d}\varepsilon^{\mathrm{p}}_{\mathrm{eff}}$ can be defined in terms of the plastic work per unit volume in the form

$$\mathrm{d}w^{\mathrm{p}} = \sigma_{\mathrm{eff}}\mathrm{d}\varepsilon^{\mathrm{p}}_{\mathrm{eff}} = \sigma_{ij}\mathrm{d}\varepsilon^{\mathrm{p}}_{ij} = \sigma_I \mathrm{d}\varepsilon^{\mathrm{p}}_{I} + \sigma_{II}\mathrm{d}\varepsilon^{\mathrm{p}}_{II} + \kappa\sigma_{III}\mathrm{d}\varepsilon^{\mathrm{p}}_{III}\,. \tag{24}$$

It follows from Eq. (24) using Eq. (8) and the results from coefficient comparison that the effective plastic strain increment is given by the following equation

$$\mathrm{d}\varepsilon^{\mathrm{p}}_{\mathrm{eff}} = \frac{1}{\sigma_{\mathrm{eff}}}\left[\sigma_I \mathrm{d}\varepsilon^{\mathrm{p}}_{I} - \sigma_{II}\frac{1}{E}(-\nu\mathrm{d}\sigma_I + \mathrm{d}\sigma_{II} - 2\kappa\nu\mathrm{d}\sigma_{III}) - \kappa\sigma_{III}\frac{1}{E}(-\nu\mathrm{d}\sigma_I - \nu\mathrm{d}\sigma_{II} + \mathrm{d}\sigma_{III})\right]. \tag{25}$$

It should be mentioned here that the elastic range is independent of the yield criterion and the following incremental relation can be derived for the uniaxial strain case:

$$\frac{\mathrm{d}\sigma_I}{\mathrm{d}\varepsilon_I} = K + \frac{4}{3}G\,, \tag{26}$$

where $K+\frac{4}{3}\,G$ is known as the constrained modulus. The last equation may play an important role for the experimental determination of the elastic material parameters of cellular materials. If Young's modulus E is obtained from a uniaxial tensile or compression test, then Poisson's ratio ν can be calculated from the slope $\frac{\mathrm{d}\sigma_I}{\mathrm{d}\varepsilon_I}$ in the elastic range of an axial compression test. Using the well-known relationships between elastic constants (e.g. (Chen and Hahn, 1988)), Eq. (26) can be rewritten as:

$$\frac{\mathrm{d}\sigma_I}{\mathrm{d}\varepsilon_I} = \frac{E}{3(1-2\nu)} + \frac{4}{3}\cdot\frac{E}{2(1+\nu)}\,. \tag{27}$$

The plane strain test reveals also an interesting relationship for the elastic range. Introducing $\varepsilon^{\mathrm{e}}_{II} = 0$ and $\sigma_{III} = 0$ into Hooke's law, a new equation for the determination of Poisson's ratio is obtained:

$$\nu = \frac{\sigma_{II}}{\sigma_I}\,. \tag{28}$$

It should be highlighted here that the application of Eq. (28) requires only force measurement to determine the stresses and is independent of any strain measurement.

4. Results

4.1 Plane strain test

For the verification of the determination of Poisson's ratio based on Eq. (28), tests on solid materials with known elastic constants were performed (cf. Fig. 4, left)). For the cubic solid sample made of the transparent plastic PMMA, the same value of Poisson's ratio could be determined based on strain gauge measurements and evaluation of the plane strain experiments. The second material was a rubber-based composite material and it is known that Poisson's ratio converges towards a value of 0.5.

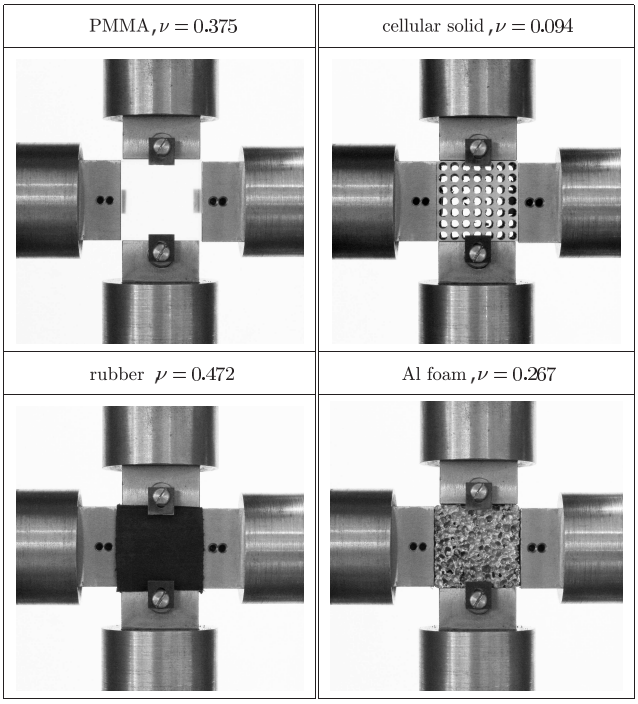

Figure 4. Determination of Poisson's ratio for solid (left) and cellular (right) materials in a biaxial testing machine

Based on the positive results from these preliminary investigations, Poisson's ratio of cellular materials was investigated. For the investigated cellular model system (cf. Fig. 4, right), a value of 0.094 was measured and the finite element

simulation was able to confirm the experimental result. In addition to this regular model material, a real aluminum foam (Alporas®) with a relative density of $\rho/\rho_S = 0.155$ was investigated. For the measured value of Poisson's ratio ($\nu = 0.267$), no comparative value from simulations is available. An averaged value of $\nu \approx 0.33$ based on experimental results (linear interpolation) is reported in (Gibson and Ashby, 1997). However, it should be emphasised here that the values reported in (Gibson and Ashby, 1997) vary strongly for small relative densities ($0.12 \leq \nu \leq 0.56$).

The progression of the uniaxial yield stress and of the parameter α which weights the influence of the hydrostatic stress on the the yield behaviour is shown in Fig. 5 for the regular model structure (tubular pores) and compared with the numerical results based on unit cells with periodic boundary conditions (MPCs) and free boundaries. It can be seen that the experimental values are between the numerical results based on the two different boundary conditions and represent the overall behaviour of the two parameters in quite a good way. Factors for the slight deviation could be the influence of the friction between the pressure feet and the specimen or the small pre-stressing at the beginning of the experiment.

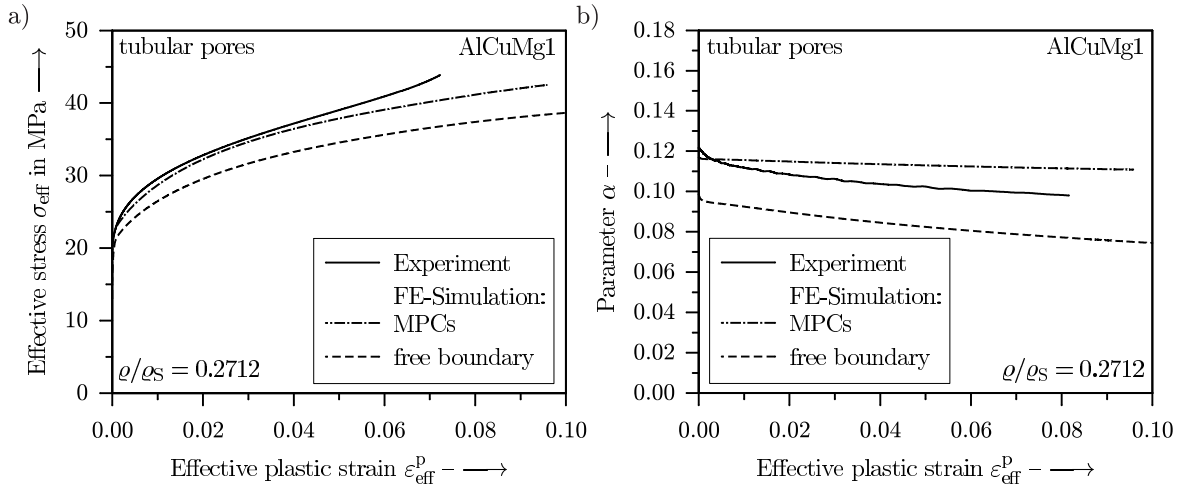

Figure 5. The dependence of the effective stress (a) and of the parameter α (b) on the equivalent plastic strain

4.2 Uniaxial strain test

In the case of the uniaxial strain test, only numerical simulations on regular structures with spherical pores were performed. The corresponding FE model for the unit cell approach with appropriate boundary conditions (3D) and a homogenised structure (axis-symmetric) are shown in Fig. 6. The geometry corresponds to a cellular structure with a relative density of $\rho/\rho_S = 0.7$.

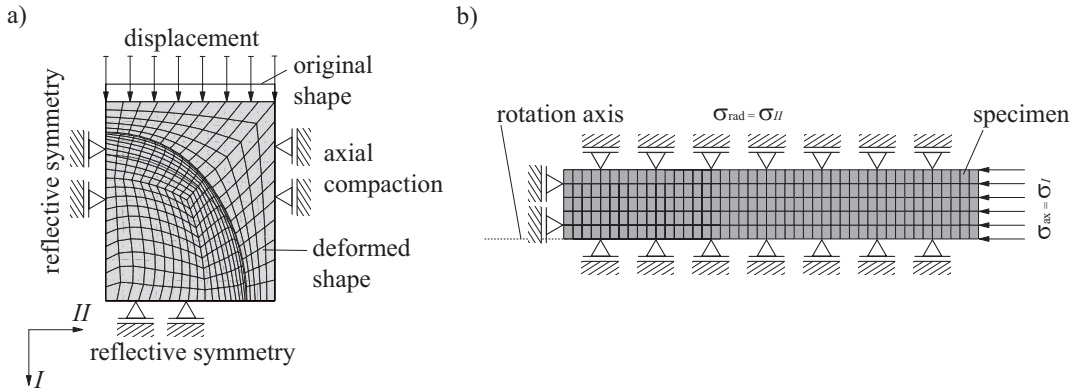

Figure 6. Uniaxial strain: a) FE model for the unit cell approach; b) illustration of the homogenised FE model

The slope of the input polynomial $\alpha(\varepsilon^p_{eff})$, gained in the unit cell approach, as a function of the equivalent plastic strain ε^p_{eff} is drawn in Fig. 7 a). In addition, α obtained by the postprocessing of the FE results of the homogenised model is visualised. Except for a minor deviation in the case of small ε^p_{eff} both slopes coincide. Consequently, it can be concluded that the homogenisation is valid under the chosen parameters.

In the physical experiment, the constraining of the axial deformation is obtained by means of a tube. This tube is characterised by a finite stiffness E_{tube} which leads to a small deformation of the specimen in the radial direction. In the

case of the idealised definition of the boundary conditions according to Fig. 6 b), this deformation has been neglected. In the following, different ratios E_{tube}/E are considered and the disturbance on the material parameter α is analysed.

The results are illustrated in Fig. 7 b). As reference values, the input polynomial $\alpha(\varepsilon^{\text{p}}_{\text{eff}})$ is drawn by the dotted line. For high ratios E_r, good coincidence with the reference can be observed. However, the deviation to the polynomial significantly increases for small values of E_{tube}, especially for low equivalent plastic strains. With increasing $\varepsilon^{\text{p}}_{\text{eff}}$, the divergence is decreasing and the slopes converge towards the exact solution.

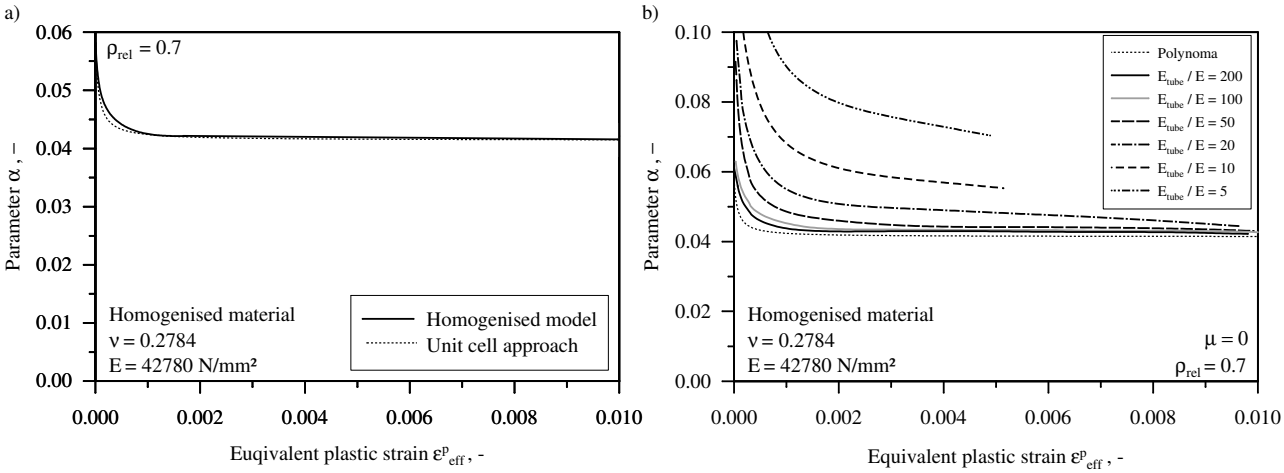

Figure 7. a) Results obtained by the uniaxial cell approach and the homogenised model; b) influence of the finite tube stiffness on the parameter α

5. Conclusions

Two new experimental techniques for porous and cellular materials, i.e. the plane stress and the uniaxial strain test, have been proposed and verified based on regular-shaped periodic cell structures. These tests aim to determine all parameters of the yield surface and allow for the determination of for example Poisson's ratio, a second elastic constant for the continuum mechanical material description.

6. Acknowledgements

The authors are grateful to Portuguese Foundation of Science and Technology for financial support.

7. References

Ashby, M.F., Evans, A., Fleck, N.A., Gibson, L.J., Hutchinson, J.W., and Wadley, H.N.G., 2000, "Metal Foams: A Design Guide", Butterworh-Heinemann, Boston, USA.

Chen, W.F. and Hahn, D.J., 1988, "Plasticity for structural engineers", Springer, New York.

Deshpande, V.S. and Fleck, N.A., 2000, "Isotropic models for metallic foams", J. Mech. Phys. Solids, Vol.28, pp. 1253-1283.

Deshpande, V.S. and Fleck, N.A., 2001, "Multi-axial yield behaviour of polymer foams", Acta Mater., Vol.49, pp. 1859-1866.

Gibson, L.J. and Ashby, M.F., 1997, "Cellular solids", Cambridge University Press, Cambridge, UK.

Körner, C. and Singer, R.F., 2000, "Processing of Metal Foams - Challenges and Opportunities", Adv. Eng. Mater., Vol.2, pp. 159-165.

Mahrenholtz, O. and Ismar, H., 1979, "Ein Modell des elastisch-plastischen Übergangsverhalten metallischer Werkstoffe", Abh. Braunschweig. Wissen. Gesell., Vol.30, pp. 138-144.

Mahrenholtz, O. and Ismar, H., 1981, "Zum elastisch-plastischen Übergangsverhalten metallischer Werkstoffe", Ing-Archiv, Vol.50, pp. 217-224.

Ströhla, S., Winter, W. and Kuhn, G., 2003, "Modeling of the elastic-plastic transition region in metal foams", Proceedings of the 1. Workshop on Advanced Computational Engineering Mechanics, Maribor, Slovenia, pp. 83-90.

Ströhla, S., Winter, W. and Kuhn, G., 2004, "Yield-behavior of closed-cell metal foams in the elastic-plastic transition region", Application of Porous Media (ICAPM 2004), Évora, Portugal, pp. 417-425.